



Variations in stem radii of *Larix principis-rupprechtii* to environmental factors at two slope locations in the Liupan Mountains, northwest China

Jing Ma¹ · Jianbin Guo¹ · Yanhui Wang² · Zebin Liu² · Di Gao¹ · Liu Hong¹ · Ziyong Zhang¹

Received: 29 July 2019 / Accepted: 11 November 2019 / Published online: 11 April 2020
© Northeast Forestry University 2020

Abstract Relationships between stem growth and climatic and edaphic factors, notably air temperatures and soil moisture for different slopes, are not completely understood. Stem radial variations were monitored at the bottom and top slope positions in a *Larix principis-rupprechtii* plantation during the 2017 and 2018 growing seasons. Total precipitation during the growing season in 2017 and 2018 was 566 mm and 728 mm, respectively. Stem contractions typically occurred after mid-morning followed by swelling in the late afternoon in both plots, reflecting the diurnal cycle of water uptake and loss. Trees at the two locations showed the same growth initiation (mid-May) because of the small differences in air and soil temperatures. There were no significant differences in cumulative stem radial growth between the bottom plot (1.57 ± 0.34 mm) and the top plot (1.55 ± 0.26 mm) in 2018.

However, in 2017, the main growth period of the bottom plot ceased 17 days earlier than in the top plot, while cumulative seasonal growth of the bottom plot (1.08 ± 0.25 mm) was significantly less than the top plot (1.54 ± 0.43 mm). Maximum daily stem shrinkage was positively correlated with air and soil temperatures, solar radiation, vapor pressure deficits, and negatively correlated with volumetric soil moisture content. The maximum daily shrinkage reflected transpiration rates as affected by environmental factors. Daily radial stem increment was correlated with precipitation and volumetric soil moisture in both years, but with air temperatures only in 2017. The seasonal growth of *L. principis-rupprechtii* Mayr thus shows interannual dynamics, while precipitation constitutes a key driving factor.

Keywords Stem radial variations · Main growth period · Diurnal patterns · Initiation temperatures · Meteorological factors · *Larix principis-rupprechtii* plantation

Project funding: The work was supported by the Ningxia Hui Autonomous Region (QCYL-2018-12), the National Key Research and Development Program of China (2016YFC0501603 and 2017YFC0504602), and the National Natural Science Foundation of China (41671025).

The online version is available at <http://www.springerlink.com>

Corresponding editor: Tao Xu.

Electronic supplementary material The online version of this article (<https://doi.org/10.1007/s11676-020-01114-w>) contains supplementary material, which is available to authorized users.

✉ Jianbin Guo
jianbinguo@bjfu.edu.cn

¹ School of Soil and Water Conservation, Beijing Forestry University, Beijing 100083, People's Republic of China

² The Research Institute of Forest Ecology, Environment and Protection, Chinese Academy of Forestry, Beijing 100091, People's Republic of China

Introduction

Recent climate changes, particularly warming and extreme drought, have considerable effects on tree growth in semiarid areas (Boisvenue and Running 2006). A number of studies have concluded that increasing temperatures and changing precipitation regimes affect seasonal growth patterns (Ciais et al. 2005; Deslauriers et al. 2007). Considerable progress has been made in dendroclimatological studies of tree growth and response to meteorological factors at annual or multiyear scales (Gou et al. 2005; Shrestha et al. 2017). However, these studies do not fully explain the consequences of environmental changes on tree growth (Gruber et al. 2009; Gutiérrez et al. 2011) and do not capture seasonal growth variabilities and relevant growth-limiting

factors (Fritts 1976). This is because tree growth is affected by environmental factors not only at yearly scales, but also at diurnal or short-time scales (Taschler and Neuner 2004; Adams and Kolb 2005; Liu et al. 2013). Therefore, it is useful to recognize and quantify daily responses of tree radial growth to environmental factors. Traditional dendroclimatology studies are not ideal for interpreting short-term growth responses to changing environmental factors due to their low time resolution.

Simultaneous and high-resolution monitoring of stem radii and environmental conditions, e.g., weather parameters and soil moisture, can provide a basis to improving an understanding of tree growth responses to climate change (Rossi et al. 2006; Michelot et al. 2012). For such studies, automatic dendrometers continually monitor radial variations of tree stems with a high time resolution (e.g., in hours or minutes), and have been increasingly applied at daily and seasonal scales (Herzog et al. 1995; Biondi and Hartsough 2010; Deslauriers et al. 2011; Dong et al. 2012). For example, it has been reported that diurnal stem radii variations consist of the irreversible growth of new xylem cells and reversible stem shrinkage and swelling (King et al. 2013; Zweifel et al. 2016; Mencuccini et al. 2017), and were divided into contraction, recovery and increment phases according to Downes et al. (1999) and Deslauriers et al. (2003). Seasonal stem radial variation has been divided into several stages according to growth changes. For example, Vieira et al. (2013) divided the seasonal cycle into five periods: winter dormancy, spring growth, pre-summer contraction, summer quiescence and autumn re-hydration. Liu et al. (2017a) however, divided it into three distinct stages, including most rapid and continuous radius increment (stage 1), persistent radius shrinkage (stage 2), and minimum stem radius growth (stage 3). The most growth occurs in the main growth period, which is considered as the primary stage to clarify the relationship between tree growth and environmental factors (Tian et al. 2017; Xiao et al. 2018).

Slope plays an important role for the redistribution of environmental resources and leads to different growth conditions for trees positioned along the slope (Lu et al. 2012). Brunori et al. (1995) investigated the growth of *Eucalyptus occidentalis* Endl. and *E. sargentii* Maiden at different slope positions and aspects. The results showed that trees on the mid-slope had the lowest above-ground biomass and stem biomass compared with other slope positions after seven years in Dudaïm, Negev Desert of Israel. Jiang et al. (2015) reported that trees on the upper distribution limit had shorter growing seasons but higher maximum growth rates, compared with trees on the lower distribution limit which had longer growth periods with lower maximum growth rates. Pärn (2003) carried out a study of *Scots pine* in southwest Estonia and found different radial growth rates of trees between the top and foot of the slope. Similarly, Lu

et al. (2012) found that the diameter at breast height (DBH), height and volume growth of *Manglietia glauc* were highest in the bottom slope, then mid-slope, and lowest in the upper slope, both in its original location, Báo Yên of Lào Cai, Vietnam, and on introduced sites in Guangxi, China. The reasons for differences of tree growth on slopes may be related to different growth strategies of trees at different slope positions, to the start and finish of growing season, and to different growth sensitivities to environmental factors. However, systematic research on reasons for differences of tree growth at different slope positions remains poor and the environmental impacts are not completely understood, especially over short-time periods such as hourly or daily scales. This limits further understanding of spatial patterns of tree growth along slopes.

Liupan Mountain, located in the northwest of the Loess Plateau, is an important source of water. This area is a special geographical location, not only because it is a transition area from semi-arid to semi-wet regions, but it is also a transition area from loess (fertile, wind-blown silt deposits) to Rocky Mountains area. It has large inter-annual wetness fluctuations and climate gradients. The plantations in this study has high forest cover, accounting for 31.3% of the area, and are mainly pure stands *L. principis-rupprechtii* (approximately 90% of the total plantations). They play an important role in soil and water conservation and in wood production (Liu et al. 2017a). The impacts of environmental factors on radial growth are important for vegetation restoration in this region. In addition, spatiotemporal variations of environmental factors on mountain slopes are complex. Liu et al. (2017a, 2018) reported that there was a remarkable variation in soil moisture along slope positions. Li (2014) found that evapotranspiration gradually increased with decreasing slope. These variations will lead to different growth indexes among slope positions. For example, Guan (2007) reported that the average growth rate of the ground stem diameter (15 cm above ground) was faster on the middle slope and slowest on the bottom slope in semi-arid areas of the Liupan Mountain. Biomass increased first, then decreased along slope positions, reaching a maximum at the middle-upper slope (Wang et al. 2015a, b).

However, do the start and finish of the main growth period and the cumulative radial growth at different slope positions coincide? How does stem radial growth respond to environmental factors at different slope positions? These questions are still unanswered. Previous studies mainly focused on the environmental controls of stem radial growth at one slope position; relatively few studies have been carried out at different slope positions. This has an impact on scientific afforestation and forest management. In addition, simulating or predicting the impact of climate change on tree growth is of major interest (Pompa-García et al. 2017; Campelo et al. 2018), and the same

is true for researches of *L. principis-rupprechtii* growth (Liu 2009; Xiong et al. 2007). However, the influence of environmental conditions on tree growth is different along slope positions, which may lead to errors in simulating or predicting the effects of climate change on the growth of *L. principis-rupprechtii*. Therefore, it is important to clarify *L. principis-rupprechtii* growth at different slope positions.

In this study, the daily radial growth of *L. principis-rupprechtii* and primary environmental factors at bottom and top positions were monitored in the 2017 and 2018 growing seasons using a high resolution automatic band dendrometer on a southeast-facing slope of the semi-humid Liupan Mountain. The objectives were: (1) to determine diurnal and inter-annual growth variation patterns of stem radii of *L. principis-rupprechtii*; (2) to explore the relationship between radius variations and environmental factors during the growth period at bottom and top on a slope; and, (3) to determine maximum daily shrinkage (MDS), maximum daily recovery (MDR) and daily radial increment (SRI) to environmental factors. This research may provide better understanding of environmental factors driving *L. principis-rupprechtii* growth on slopes and assist to predict growth response to climate change.

Materials and methods

Study area

The study area was the small watershed of Xiangshuihe ($35^{\circ}15'–35^{\circ}41' N$, $106^{\circ}09'–106^{\circ}30' E$) in the southern area of the Liupan Mountains (Fig. 1). The area is 2070–2931 m a.s.l., approximately 43.7 km² and with a semi-humid, warm temp climate. Annual mean temperature is 5.8 °C, and mean annual precipitation 618 mm (1981–2010). Soils are gray-brown and alpine meadow soils with a high gravel content and an average thickness of approximately 80 cm (Liu 2011).

The site was a representative southeast-facing slope covered by pure *L. principis-rupprechtii* and carried out during May–Oct growing seasons of 2017 and 2018. The slope had a gradient of approximately 30°, elevation of 2271–2480 m a.s.l. and a horizontal length of 425.1 m. A bottom plot and a top plot were selected for study (Fig. 1; supplementary Fig. S1). The plots 30 m × 30 m and trees were 36 years-of-age in 2017. Mean DBH, soil bulk density, total porosity, and maximum water-holding capacity in the top plot were greater than in the bottom plot (Table 1). Tree growth traits (DBH and biomass) of bottom and top plots showed large differences (Liu 2018).

Fig. 1 Study area, study slope, and study plots (TP and BP represent the top plot and the bottom plot on the study slope, respectively)

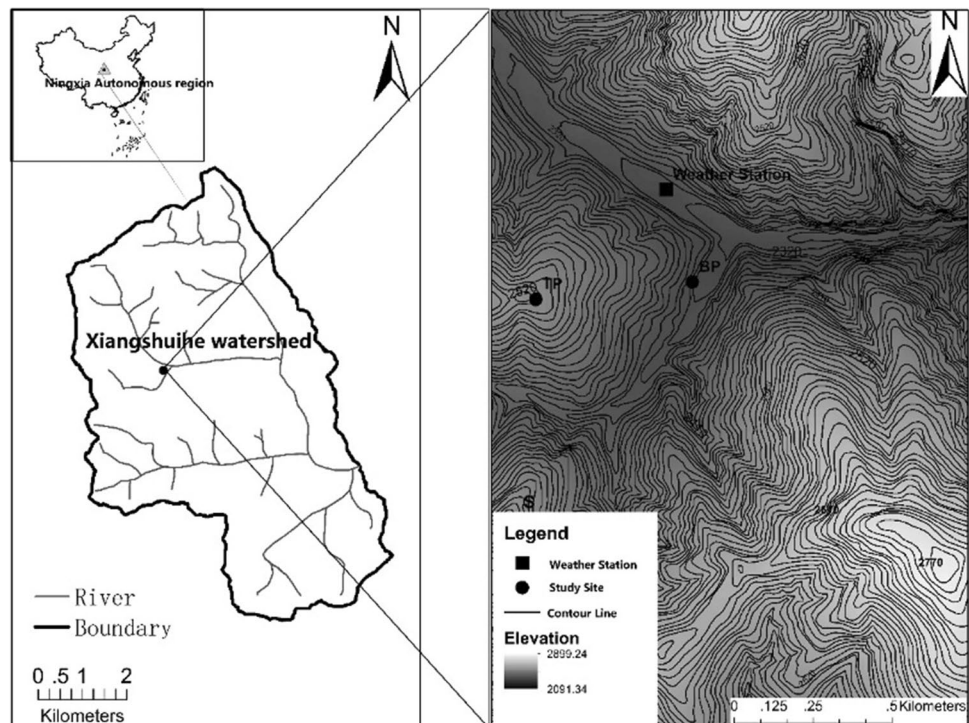


Table 1 Stand and site characteristics of bottom and top plots

Factors	Parameters	Bottom plot	Top plot
Site conditions	Elevation (m)	2275	2471
	Slope gradient (°)	34.9	26.3
	Slope aspect	Southeast	Southeast
	Distance from slope top (m)	425.1	26.9
Vegetation	Canopy density	0.72	0.73
	Stand density (stems ha ⁻¹)	907	942
	Mean tree height (m)	16.19 ± 2.34	16.77 ± 1.76
	Mean DBH (cm)	18.71 ± 4.03	20.25 ± 3.59
	Mean crown diameter (m)	3.27 ± 0.81	3.21 ± 0.71
Soil physical properties	Biomass (t ha ⁻¹)	120.78	136.61
	Soil bulk density (g cm ⁻³)	0.94	0.98
	Total porosity (%)	56.3	59.0
	Maximum water-holding capacity (%)	57.6	64.3

Data collection

Dendrometer record collection

Four healthy trees with different diameters were selected as samples based on DBH classes of all trees within each plot, and each tree selected represented one of four DBH classes present. The characteristics of the sample trees are shown in Table 2. Automatic band dendrometers (DC2, Ecomatik, Munich, Germany) were installed on sample trees during the May to October growing season in 2017 and 2018. The principle of the band dendrometer is the relationship between the resistance of the sensor and the instant tension expressed to determine changes in stem shrinking and swelling (Xiong et al. 2007). The circumference growth of four sample trees in each plot were continuously monitored at 1.3 m above the ground using an automatic band dendrometer with a resolution of 2 µm and a temperature coefficient < 0.1 µm K⁻¹. Data were collected every 5-min, but averaged per half-hour and stored in a data logger (DL15, Ecomatik, Munich). To minimize the interference caused by the expansion and contraction of the bark, dead bark was removed without

wounding the cambium. The dendrometer sensor was then fixed on the trunk with a wire of plastic beads and a rubber belt. The functions of the plastic beads were to reduce the friction between the wire and stem and to avoid direct contact between the wire and trunk.

Weather conditions and soil moisture records collection

Weather data of the bottom and top plots were collected using an automatic meteorological station (WeatherHawk 232, WeatherHawk, Logan, UT, USA). One was located at the top of the slope, and the other was in a relatively flat open area outside the plantation, approximately 100 m from the slope. The weather data included air temperatures (Ta, °C), relative humidity (RH, %), precipitation (P, mm), solar radiation (R, W m⁻²) and wind speed (Ws, m s⁻¹), all recorded at 5-min intervals. Because the altitude of the position of the weather station outside the bottom plot was similar to that of the plot, the stand crown was assumed to be the same. The vapor pressure deficit (VPD, kPa) was calculated from the site-specific Ta, RH and air pressure

Table 2 Characteristics of sample trees for the monitored stem variation

Plot	Tree Number	DBH (cm)	Tree height (m)	Clear bole height (m)	Crown diameter (m)
Bottom plot	1	14.29	13.80	5.80	3.84
	2	17.60	16.80	6.50	4.29
	3	21.19	17.00	6.00	4.67
	4	21.81	20.50	6.40	5.78
Top plot	1	15.63	16.00	9.00	4.71
	2	20.00	16.60	6.90	6.70
	3	22.29	19.50	6.30	5.00
	4	25.30	19.10	5.10	5.94

values for all the sites using the equation below (Campbell and Norman 1998):

$$VPD = 0.611 \times \left(1 - \frac{RH}{100}\right) \times e^{\frac{17.502 \times T_a}{T_a + 240.97}} \quad (1)$$

The volumetric soil moisture (VSM, m³ m⁻³) and soil temperatures (Ts, °C) of each plot were monitored using electrical conductivity sensors (5TE, Decagon, Washington, DC, USA) at a location close to the sample trees. The distribution of the roots was concentrated in the upper 60-cm soil layer (Liu et al. 2017b). The volumetric soil moisture for the root zone has a vital role in tree growth, and transpiration directly affects soil moisture in the main root zone (Han et al. 2019). Therefore, the volumetric soil moisture of the upper 60 cm was focused on this layer. The sensors were buried into the upper 10-cm, 10–20, 20–40, and 40–60 cm layers. Data were stored at 30-min intervals in data logger (Em50, Decagon). Weighted averages of soil moisture and temperatures in the upper 60 cm layer were obtained using the soil thickness of each soil layer as a weight factor.

Statistical analysis

Extraction of stem radial changes

Mean DBHs were 18.7 ± 3.5 and 20.8 ± 4.1 cm (means ± standard deviation) and mean tree heights were 17.0 ± 2.7 and 17.8 ± 1.8 m for sample trees in the bottom and top plots, respectively. These values were close to the mean DBH and height of the plots. Therefore, the averages of four sample trees of each plot were analyzed. The circumference dendrometer data were converted into radii data for additional comparison and analysis. To compare the radial increments among the four sample trees, the first value recorded on the first day was set to

zero for all the trees (Tardif et al. 2001). The stem radius variation was divided into three phases: (1) the contraction phase, the period between the first maximum radius and the subsequent minimum; (2) the recovery phase, the period between the minimum radius and the previous maximum radius; and, (3) the increment phase, the period from the previous maximum to the subsequent maximum radius (Downes et al. 1999; Deslauriers et al. 2003). The daily variations of the stem radius are shown in Fig. 2. According to these phases, the maximum daily shrinkage (MDS), maximum daily recovery (MDR), and daily stem radial increment (SRI) were obtained from each sample tree. Figure 2 shows that the magnitude and the duration of SRI clearly increased on some days but do not reflect actual growth. Instead, they were caused by the swelling of the bark due to heavy rainfall. Therefore, these data were excluded during the analysis. The amplitudes and relative durations of these three phases and the corresponding environmental factors of these phases in each circadian cycle were calculated using the “dendrometeR” package (Deslauriers et al. 2011) in R 3.3.3 software (R Development Core Team, Vienna, Austria) (Ernst et al. 2016).

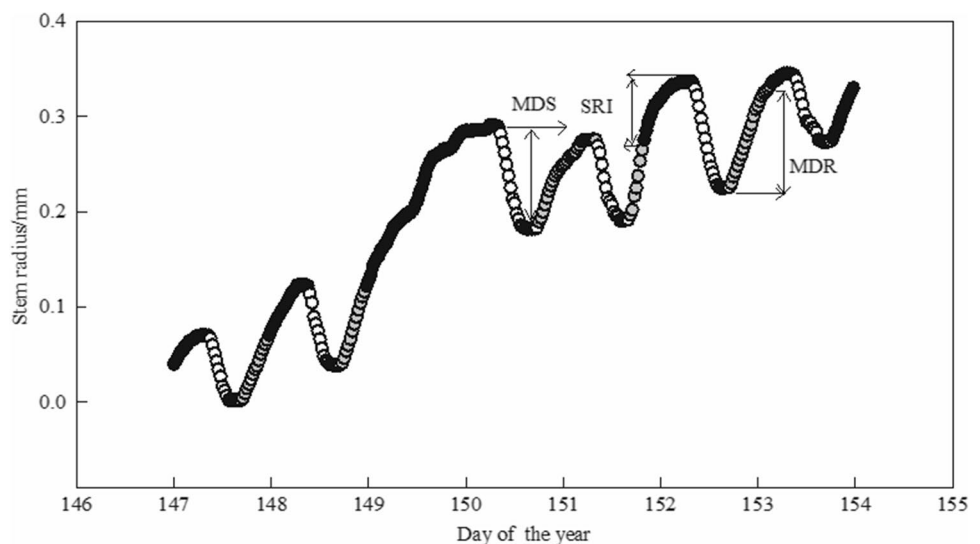
Determination of the main growth period

The Gompertz model was used to simulate the daily mean series of the stem radius in each of the two plots. The data to be processed were the averages of four sample trees in each plot. The simulation period was from May to October in 2017 and 2018, respectively. The Gompertz function (Deslauriers et al. 2003; Duchesne et al. 2012) is as follows:

$$Y = A * \exp(-\exp(-k * (x - b))) \quad (2)$$

where Y is the daily averaged measurement of the stem radius (mm); A is the upper asymptote; b is a parameter

Fig. 2 The circadian cycle of stems divided into three distinct phases



related to the initial value of x ; k is the rate of change parameter, and x is the time in days (day of the year (DOY)).

Radial growth rate curves were obtained by calculating the first derivative of the simulated functions. Based on the dendrometer accuracy ($\pm 2 \mu\text{m}$) and the growth rate in different periods, the initiation and end of the main growth period were defined as the time when the modeled daily growth rates exceeded or fell below 0.004 mm/day (Lu 2016; Tian et al. 2017). Values from the main growth period were used for the subsequent growth (diurnal and interannual)—environment correlation analysis.

Correlation analysis of the MDS, MDR, SRI and environmental factors

Since the MDS and SRI were non-normally distributed, non-parametric Spearman correlation coefficients were applied using SPSS 20.0 software (IBM Inc., Chicago, IL, USA) to quantify the relationships between the MDS, MDR, SRI and daily environmental variables, including precipitation (P , mm), air temperature (T_a , $^{\circ}\text{C}$), relative humidity (RH, %), solar radiation (R , W m^{-2}), vapor pressure deficit (VPD, kPa), volumetric soil moisture (VSM, $\text{m}^3 \text{m}^{-3}$), and soil temperature (T_s , $^{\circ}\text{C}$). The differences were analyzed by one-way analysis of variance (ANOVA) and further by multiple comparisons (LSD) using SPSS 20.0.

Results

Environmental variables during the growing season

Meteorological conditions

The daily variations of weather parameters during the growing seasons in 2017 and 2018 are shown in Fig. 3. Annual precipitation first increased and then decreased in both 2017 and 2018. The total precipitation during the growing season in 2017 was 566 mm, and the two heaviest daily precipitation events occurred June 4 and July 5 with 40 mm and 33 mm, respectively. However, the total precipitation during the growing season in 2018 was 728 mm during the study period. Daily precipitation increased sharply in the period June 24 to July 10, and extreme precipitation events occurred June 25 and July 10 with 59 mm and 60 mm, respectively. The pattern of variation in daily mean temperature was similar to that of daily precipitation, in that it increased and then decreased in both 2017 and 2018. Daily mean air temperatures of the top plot and bottom plot varied in the range of -0.3 to $20.6 \text{ }^{\circ}\text{C}$ and 0.6 to $20.5 \text{ }^{\circ}\text{C}$ in 2017, while 0.8 to $17.1 \text{ }^{\circ}\text{C}$ and 0.8 to $20.0 \text{ }^{\circ}\text{C}$ in 2018, respectively. The air temperature was similar before July 19 in 2017 and before June 24 in 2018, then became higher in the bottom plot.

The daily mean solar radiation in 2017 was 81.7 W m^{-2} and 114.5 W m^{-2} in the top and bottom plots, respectively. However, it was 68.7 W m^{-2} and 114.0 W m^{-2} in the same plots in 2018, respectively. The mean VPD fluctuated substantially during the main growth period, and its degree of variation decreased after mid-August in both years. The daily average vapor pressure deficit (VPD) in the bottom plot (0.36 kPa in 2017 and 0.28 kPa in 2018) was lower than in the top plot (0.54 kPa in 2017 and 0.53 kPa in 2018) for the duration of the growing season. During the growing period, average daily relative humidity was 77.8% in the top plot and 69.4% in the bottom plot, respectively, in 2017. However, it was 79.2% in the top and 68.3% in the bottom plots in 2018.

Soil water and soil temperature

The daily variation of volumetric soil moisture and soil temperature of the upper 60-cm soil layer in the two plots during the growing seasons in 2017 and 2018 are shown in Fig. 4. The mean volumetric soil moisture during the main growth period of 2018 was 22.9% in the bottom plot and 23.5% in the top plot, higher ($p < 0.01$) than in 2017 (22.3% and 22.7%, respectively). Soil moisture showed a large fluctuation as it is influenced by precipitation. In 2017, it was higher in the top plot than in the bottom plot before 18 August (day of the year (DOY) of 230), while it was opposite DOY 230. A sharp decline in soil moisture occurred on both plots in the period 9 July to 21 August, with a minimum of 18.3% in the top plot and 18.0% in the bottom plot. In 2018, the mean volumetric soil moisture in the upper 60-cm layer on July 10 increased to 29.7% in the top plot and 25.5% in the bottom plot, respectively. This was due to the extreme precipitation events (60 mm) in 2018.

Daily mean soil temperature in 2017 was $9.3 \text{ }^{\circ}\text{C}$ and $8.9 \text{ }^{\circ}\text{C}$ in the bottom and top plots, respectively. During the main growth period from mid-May to mid-August, the daily mean air temperatures varied between 4.9 and $13.2 \text{ }^{\circ}\text{C}$ in the bottom plot, and between 4.7 and $11.7 \text{ }^{\circ}\text{C}$ in the top plot. The daily mean soil temperature in 2018 was $9.5 \text{ }^{\circ}\text{C}$ and $9.1 \text{ }^{\circ}\text{C}$ in the bottom plot and in the top plot, respectively. During the main growing period in 2018, soil temperatures ranged from 4.8 to $13.7 \text{ }^{\circ}\text{C}$ and from 4.9 to $13.1 \text{ }^{\circ}\text{C}$ in the bottom plot and in the top plot, respectively.

Estimation of the main growth period at two locations on the slope

Radial growth curves and radial growth rates were simulated (Fig. 5). At both locations in both years, the seasonal pattern of radial variation was characterized by a gradual increase in mid-May, followed a sharp increase in early summer (June to July), and finally levelling off in autumn (August to October). The shrinkage of stem

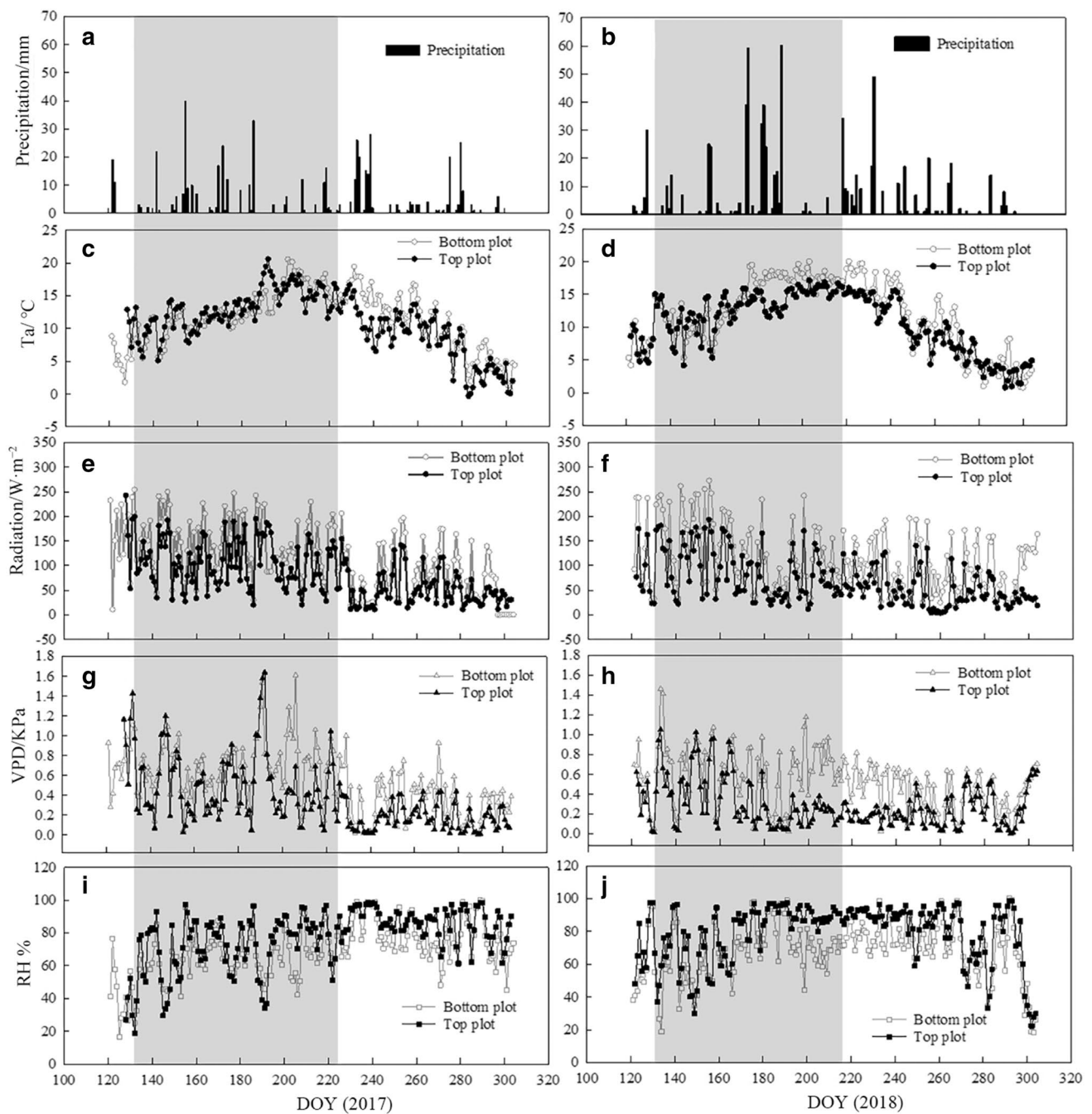


Fig. 3 Daily weather variations: precipitation (a, b), mean air temperature (c, d), solar radiation (e, f), vapor pressure deficit (g, h) and relative humidity (i, j) in bottom plot and top plot from May to October in 2017 and 2018. The shaded regions indicate the main growth periods

radii was observed from late July to mid-August in 2017. The main growth period started around mid-May in both years, however, the cessation of growth ranged from 26 July to 12 August (DOY 207–224) in 2017, and from early August in 2018 (Table 3, Fig. 5). The average duration of the main growth period in the top plot was longer than for the bottom plot in 2017, but it was similar between both plots in 2018.

Fitted models explain 93% and 98% of stem radial variation in bottom and top plots, respectively, in 2017, and 97% and 98%, respectively, in 2018, indicating that Gompertz model can accurately simulate radial growth curves during the growing season (Fig. 5a, b). The average cumulative seasonal growth in the bottom plot (1.08 ± 0.25 mm) was significantly smaller ($p < 0.01$) than in the top plot (1.54 ± 0.43 mm) in 2017, but not significantly different

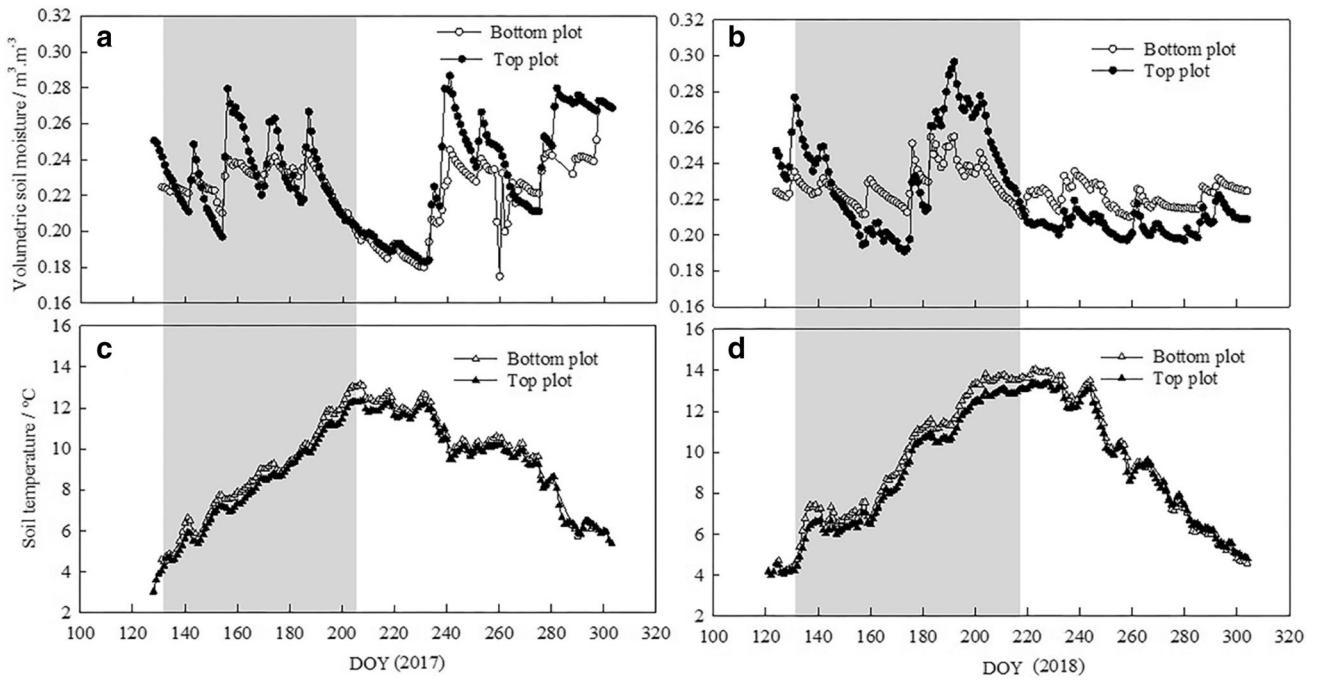


Fig. 4 Daily variation of volumetric soil moisture (a, b) and soil temperature (c, d) of the upper 60-cm soil layer on the two study plots from May to October in 2017 and 2018. The shaded area indicate the main growth periods

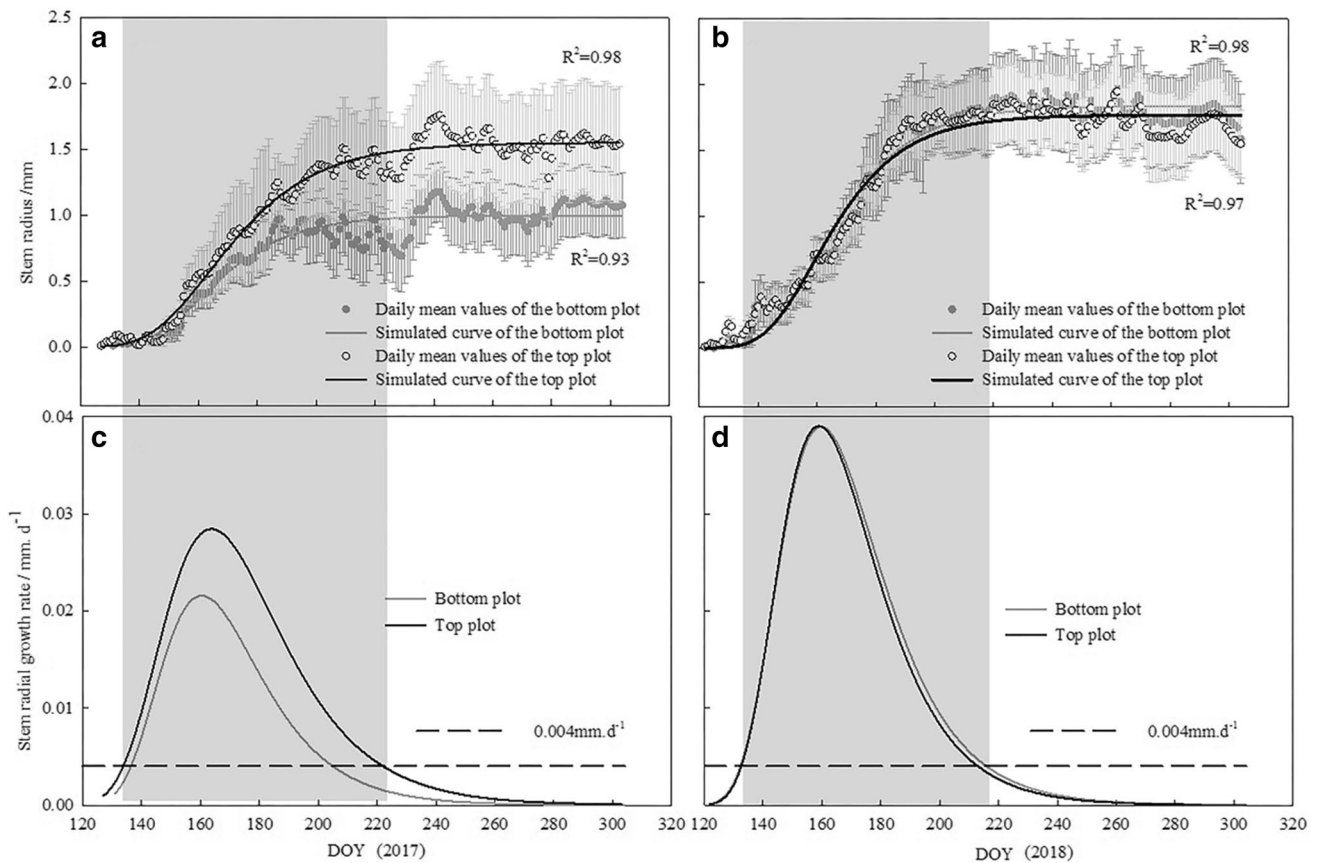


Fig. 5 Gompertz function modeled radial variations (a, b) and daily radial growth rate curves (c, d) at two plots from May to October in 2017 and 2018. Error bars indicate mean \pm SD. The shaded regions indicate the main growth periods

Table 3 Growth onset and ending; cumulative radial growth during the main growth period in 2017 and 2018

Years	Plots	Onset of main growth period (DOY)	Ending of main growth period (DOY)	Growing season length (Days)	Cumulative seasonal growth (mm)
2017	Bottom plot	136	207	72	1.08 ± 0.25
2017	Top plot	133	224	92	1.54 ± 0.43
2018	Bottom plot	132	218	87	1.57 ± 0.34
2018	Top plot	133	215	83	1.55 ± 0.26

Onset and ending of stem radial growth were estimated from the Gompertz function and given as day of year (DOY)

($p > 0.05$) between the bottom plot (1.57 ± 0.34 mm) and the top plot (1.55 ± 0.26 mm) in 2018.

Response of daily stem radius to environmental variables during main growth period

The daily cumulated radius variations decreased with increased air temperatures, solar radiation and vapor pressure deficit but increased with increased relative humidity. The daily average maximum radius growth was between hours 7:30 and 9:30, and the minimum between 16:00 and 18:30 in the bottom plot. For the top plot, average maximum and minimum radius growth were between 6:30 to 8:30 and 15:00 to 18:30, respectively, (Fig. 6). There was a lag effect between minimum radial contraction and maximum environmental factors within 1–3.5 h in the top plot and 2–4 h in the bottom plot. The average amplitudes of the daily radial contractions at bottom and top plots (0.05 ± 0.010 mm and 0.04 ± 0.003 mm) in 2017 were larger ($p < 0.05$) than in 2018 (0.04 ± 0.004 mm and 0.02 ± 0.003 mm).

Correlation between stem radius and environmental factors in the growing season

The correlation varied by plots and years (Fig. 7). The maximum daily shrinkage (MDS) was positively correlated with air and soil temperatures but negatively correlated with volumetric soil moisture (VSW) at both plots in 2017. However, the MDS was positively correlated with soil radiation (R) and vapor pressure deficit (VPD), but negatively with relative humidity (RH) and VSW at both plots in 2018. The maximum daily recovery (MDR) was negatively correlated with VSW but positively with soil temperature in the top plot, and negatively correlated with the VSW in the bottom plot in 2017. The MDR was positively correlated with soil radiation and vapor pressure deficit (VPD), and negatively correlated with relative humidity and volumetric soil moisture (VSM) in the bottom plot and negatively correlated with VSM in the top plot in 2018. Stem radial increment (SRI) was positively correlated with air temperatures and VSM in the bottom plot and positively correlated with precipitation in both plots in 2017. However, the stem radial increment

was positively correlated with precipitation and volumetric soil moisture in the bottom plot, and precipitation in the top plot in 2018.

Discussion

Daily radial variation in the bottom and top plots and its response to environmental factors

The observed daily radius variations during the growing season indicated that stem diameters were largest mid-morning and smallest in the late afternoon (Fig. 6), reflecting the diurnal cycle of water uptake and loss. Due to the increase of temperature in the morning, transpiration gradually increases during the day, leading to increases in leaf water potential and decreases in cell turgor (Zhang et al. 2016). However, radiation and temperatures decrease in the evening (Fig. 6), and water transport in the xylem and turgor recovery weaken (Xiao et al. 2010). Compared with stem radius variations in the bottom and top plot, there was (1) an earlier starting time for radius contractions, and (2) a longer duration of the radius recovery phase. This was primarily because the diurnal variation of stem water storage was the consequence of the balance between water input through root uptake and water loss through transpiration (Lu et al. 2015). The mean amplitudes of daily contractions in the bottom and top plots in 2017 were larger than in 2018 due to the higher average air temperatures and lower mean volumetric soil moisture of daily contraction in 2017 (10.5 °C and 22.6%) than in 2018 (7.0 °C and 23.2%). For different slope positions, the higher mean air temperature and lower mean volumetric soil moisture of daily contractions were in bottom plot (8.0 °C and 22.9%) compared with those in the top plot (6.1 °C and 23.5%) in 2018. Therefore, the mean amplitude of daily contractions in the bottom plot (0.035 ± 0.004 mm) was significantly higher than in top plot (0.022 ± 0.003 mm) in 2018. The higher amplitude of daily contractions corresponded to higher air temperatures and lower soil moisture, indicating that stem shrinkage was caused by soil water deficits resulting from high transpiration driven by high temperatures (Liu et al. 2017a).

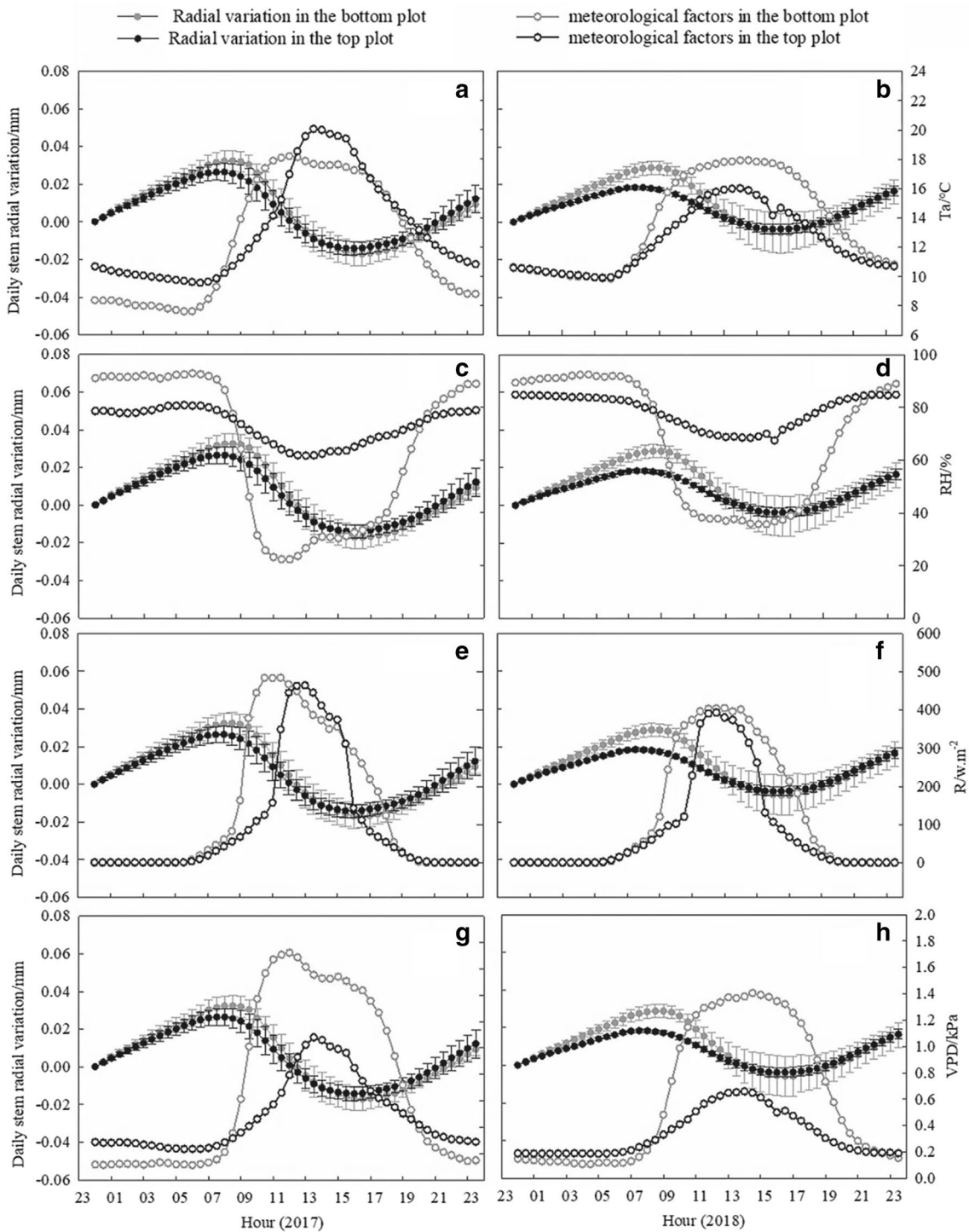


Fig. 6 Mean hourly variations of stem radius and environmental factors (air temperature (a, b), relative humidity (c, d), solar radiation (e, f), and vapor pressure deficit (g, h) for the two plots during the growing season in 2017 and 2018. Error bars indicate mean \pm SD

The bottom plot had lower average tree heights and DBHs compared with those in the top plot, which may lead to lower transpiration and weaker evaporation capacity in the bottom plot. This result is supported by the observation that stand transpiration in May to August (the main growth period) was

higher in the top plot than in the bottom plot, with average values of 29.4 ± 7.8 mm and 26.5 ± 7.7 mm, respectively (Liu 2018). In addition, there was a time lag between minimum radial contraction and maximum environmental factors with longer times (2–4 h) in the bottom plot than in the top

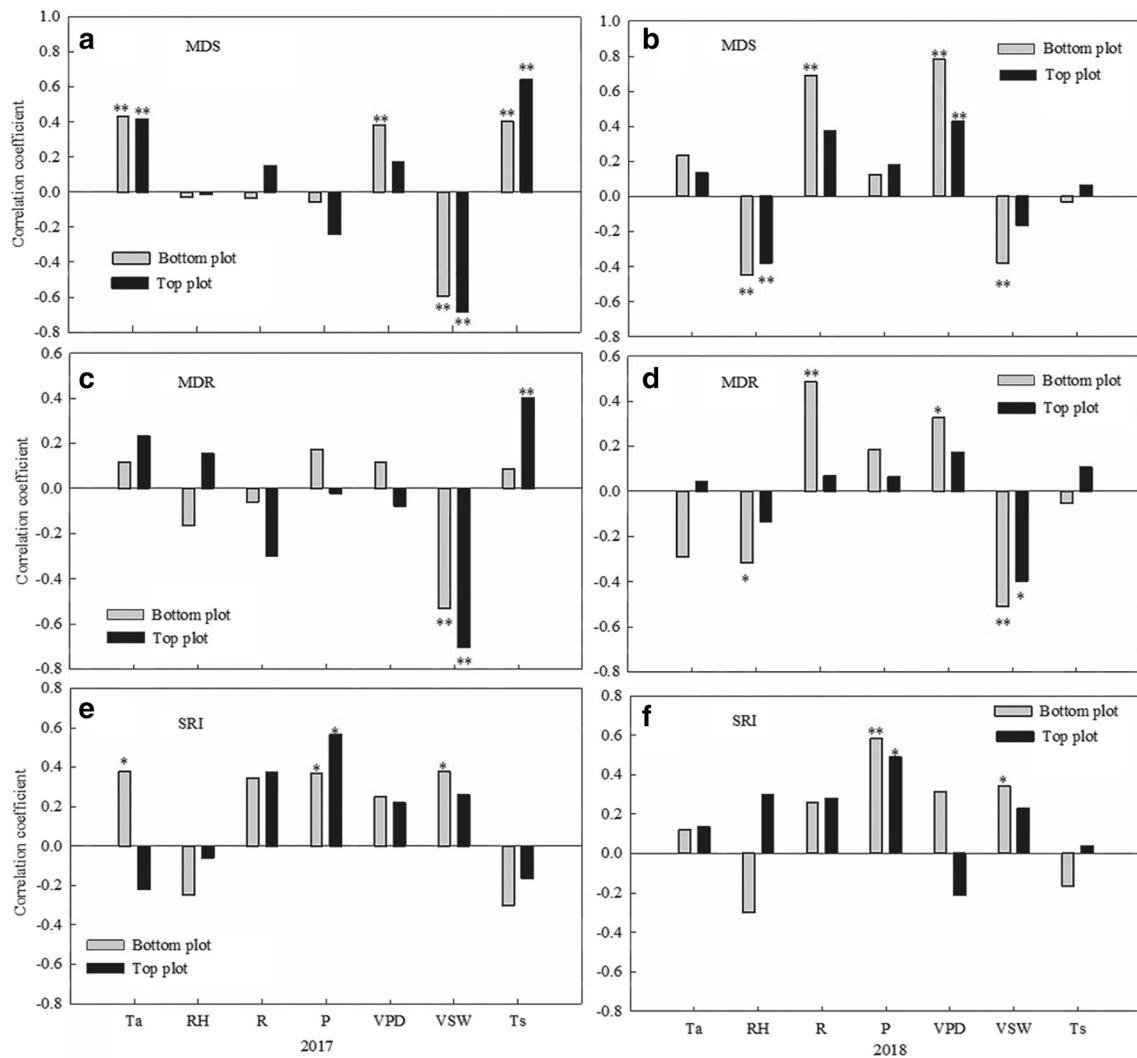


Fig. 7 Spearman correlation coefficients between daily stem radial changes: maximum daily shrinkage (a, b), maximum daily recovery (c, d), daily radial increment (e, f) and main environmental factors in 2017 and 2018. Ta is the daily mean temperature; RH is the relative

air humidity; R is the solar radiation; VPD is the vapor pressure deficit; P is precipitation; VSM is the volumetric soil moisture, and Ts is the soil temperature * $p < 0.05$; ** $p < 0.01$

plot (1–3.5 h). Therefore, average air temperatures, relative humidity, and solar radiation as well as vapor pressure deficit in the bottom plot were higher than in the top plot when stems started to contract. This may be caused by lower transpiration and weaker evaporation in the bottom plot.

Seasonal growth patterns in the two plots

In this study, stem radial growth of *L. principis-rupprechtii* started around mid-May in both years but the end date ranged from late July to mid-August (Fig. 5). Figure 4 shows that soil moisture at the time of growth initiation was 23.2% in the bottom plot and 26.2% in the top plot in 2018. However, the beginning of the main growth period in the bottom

plot was basically the same as in the top plot, indicating that soil moisture was not a factor affecting the start time.

The radial growth began only when air and soil temperatures were above certain thresholds. Previous studies found that temperature was the most important factor limiting the initiation of growth (Turcotte et al. 2009; Wang et al 2015a, b) because xylogenesis, i.e., the wood formation process, was active when the mean daily temperatures reached a certain level (Rossi et al. 2007; Tian et al. 2017). High air temperatures may lead to a remarkably high rate of cell production at the beginning of the growing season (Deslauriers and Morin 2005). On the study slope, the air temperature at growth initiation was 7.0 °C in the bottom plot and 7.8 °C in the top plot in 2017, and in 2018, 8.1 °C and 8.2 °C, respectively. This is in agreement with

Rossi et al. (2007) that mean daily temperatures of 5.6–8.5 °C was needed for the onset of wood formation. Compared with the air temperature, soil temperature is also important for cambial reactivation (Dufour and Morin 2013). Soil warming can alter the characteristics of xylem differentiation and improve the rate of cell differentiation. A study by Jiang et al. (2015) on intra-annual radial growth of *L. principis-rupprechtii* in the Luyashan Mountains also indicated that soil temperature determines the initiation of radial growth. In this study, soil temperature at growth initiation was 4.9 °C in the bottom plot and 4.7 °C in the top plot in 2017, and in 2018, 4.8 °C and 4.9 °C, respectively. Therefore, the trees in the two plots with different slope positions have essentially the same growth initiation time (mid-May) because of the small differences in air and soil temperatures.

Several studies have reported that summer water deficits cause cambial activity to cease prematurely (Levanič et al. 2009; Oberhuber et al. 2014). In this study, precipitation and soil moisture influenced the cessation of the main growth period. As shown in Figs. 3 and 4, precipitation on the study site was limited after 9 July in 2017, and soil moisture gradually decreased in early July, followed by a short drought period until August. Furthermore, soil moisture in the top plot was higher than in the bottom plot from May to early July. Thus, stored soil water in the top plot was slightly higher than in the bottom plot during the main growth period in 2017. Relatively high temperatures, scarce rainfall, strong transpiration, and low soil water availability led to a shorter growth period in the bottom plot compared to the top plot in 2017. Although growth cessation in 2018 appeared to be induced by higher soil temperatures in the bottom plot (13.7 °C) compared with the top plot (13.1 °C), the mean volumetric soil moisture during the main growth period was 22.9% in the bottom plot and 23.5% in the top plot, and higher than in 2017 (22.3% and 22.7%, respectively). Therefore, soil moisture was not a limiting factor for tree growth in 2018; the main growth period ceased at similar times in both plots in 2018.

The inflection point of stem radial growth, i.e., the maximum growth rate, occurred June 5th in the bottom plot and June 13th in the top plot in 2017, and on June 6th in both plots in 2018. An earlier inflection point resulted in less cumulative radial growth. Therefore, the cumulative growth in the bottom plot was less than in the top plot in 2017. Zhang (2018) reported that the inflection point arrives later when precipitation was greater and temperatures were lower. In this study, air and soil temperatures in the top plot were lower than in the bottom plot, resulting in the inflection point in the top plot occurring later than in the bottom plot in 2017.

Stem radial growth response to meteorological factors

Stem radii variations are a complex physiological process, and results from the tradeoff between water loss (e.g., transpiration) and water uptake (e.g., soil water absorption) during the growing period (Deslauriers et al. 2007; Devine and Harrington 2011). In this study, the maximum daily shrinkage (MDS) reflected tree transpiration rates as affected by environmental factors affecting the transpiration rate. Pérez et al. (2009) reported that warmer air and higher soil temperatures increase sap flow velocity and water uptake by the roots. Tian et al. (2017) noted that these temperatures increased water loss through transpiration and stem shrinkage. Wang et al. (2016) reported that high vapor pressure deficits (VPD) can increase transpiration rates, resulting in increased negative pressure in the water transportation system. Radiant heat can increase air temperatures and reduce relative humidities. In addition, high solar radiation (R) has negative effects on cell turgor and inhibits cell enlargement and growth (Pantin et al. 2012). Therefore, the maximum daily shrinkage was positively correlated related to air (T_a) and soil temperatures (T_s), vapor pressure deficits and solar radiation, and negatively related to relative humidity (RH). The negative correlation between maximum daily shrinkage and volumetric soil moisture indicates that soil water availability plays an important role in stem contraction. Under relatively insufficient soil water and transpiration stress due to low soil moisture, the trees could not compensate for the daily water loss through transpiration, and stem radius contraction would occur. Thus, maximum daily shrinkage increased as the volumetric soil moisture decreased.

The amplitude of the recovery was determined or driven by the magnitude of the contraction (Liu et al. 2017a), indicating that maximum daily shrinkage and maximum daily recovery are interdependent. Wang (2013) also reported that the amplitude of the one determined the amplitude of the other. When maximum daily shrinkage increased with decreasing soil moisture during the day, the corresponding recovery phase replenished the stem contraction by increasing the duration of the recovery (Liu et al. 2017a). This was the cause of the negative correlations between maximum daily recovery and volumetric soil moisture in both plots in both years. Soil temperatures can affect water uptake capacity of the roots, and thus regulate stem recovery (Li et al. 2014). At night, under the effect of root pressure, higher soil temperatures were in conformance with higher water replenishment rates.

Correlations between stem radial increment (SRI) and environmental factors in 2018 were different in 2017. Lower air temperature (12.5 °C) with higher a coefficient of variation (0.27) were found in the bottom plot compared to those in the top plot (13.2 °C and 0.23, respectively) in 2017. This may have enhanced the relationship between

air temperatures and stem radial increments in the bottom plot in 2017. Volumetric soil moisture in the top plot was higher than in the bottom plot, indicating that water loss did not play an important role in stem radius increment in the top plot. Therefore, stem radial increment (SRI) was not related to volumetric soil moisture in the top plot in 2017 (Fig. 7e, f).

Precipitation had a positive correlation with stem radial increment in both plots and was an important factor influencing radial growth in both 2017 and 2018. During the main growth period in the study years, the amount of precipitation in 2017 (231 mm) was lower than in 2018 (403 mm). High amounts of precipitation can reduce drought stress and cause a reduction in leaf water potential, leading to a release of low-pressure conditions in the cambium (Zweifel et al. 2006). Therefore, no significant difference was found in the cumulative seasonal growth between the two plots during the main growth period in 2018. However, with a lower precipitation in 2017, the cumulative seasonal growth in the bottom plot was much lower than in the top plot, implying that there were other factors influencing the cumulative seasonal growth. Table 1 shows that total porosity and maximum water-holding capacity in the bottom plot was lower than in the top plot. Therefore, the lower soil water in the bottom plot could not provide sufficient water for the trees, and thus a decrease in cumulative seasonal radius growth was observed. Overall, the results suggest that the seasonal growth of *L. principis-rupprechtii* has obvious interannual dynamics, and that precipitation was the key factor driving the seasonal growth but other factors varied by the year.

Conclusions

Daily variations of stem radii of *L. principis-rupprechtii* exhibit a clear diurnal pattern during the main growth period, namely, the largest stem diameters in mid-morning and the smallest in the late afternoon. Trees at the two plot locations showed the same growth initiation time (mid-May) because of small differences in air temperatures. There were no significant differences in cumulative radial growth between the bottom plot (1.57 ± 0.34 mm) and the top plot (1.55 ± 0.26 mm) in 2018. This may well be caused by large precipitation events that minimized differences in soil water levels between the two plots. However, in 2017, the cumulative seasonal growth of the bottom plot (1.08 ± 0.25 mm) was significantly less than for the top plot (1.54 ± 0.43 mm), partly because of the lower water-holding capacity of the soil of the bottom plot, as 2017 was a drier year. Thus, precipitation constituted a key driving factor for interannual dynamics of *L. principis-rupprechtii* growth.

References

- Adams HD, Kolb TE (2005) Tree growth response to drought and temperature in a mountain landscape in northern Arizona, USA. *J Biogeogr* 32(9):1629–1640
- Biondi F, Hartsough P (2010) Using automated point dendrometers to analyze tropical tree line stem growth at Nevado de Colima. *Mexico Sens* 10(6):5827–5844
- Boisvenue C, Running SW (2006) Impacts of climate change on natural forest productivity: evidence since the middle of the 20th century. *Glob Change Biol* 12(5):862–882
- Brunori A, Nair PKR, Rockwood DL (1995) Performance of two Eucalyptus species at different slope positions and aspects in a contour-ridge planting system in the Negev Desert of Israel. *For Ecol Manage* 75(1–3): 0–48
- Campbell GS, Norman JM (1998) An Introduction to Environmental Biophysics, 2nd edn. Springer-Verlag, New York, USA
- Campelo F, Gutiérrez E, Ribas M, Sánchez-Salguero R, Nabais C, Camarero JJ (2018) The facultative bimodal growth pattern in *Quercus ilex*—a simple model to predict sub-seasonal and inter-annual growth. *Dendrochronologia* 49:77–88
- Ciais Ph, Reichstein M, Viovy N, Granier A, Ogee J, Allard V, Aubinet M, Buchmann N, Chr B, Carrara A, Chevallier F, De Noblet N, Friend AD, Friedlingstein P, Grünwald T, Heinesch B, Keronen P, Knohl A, Krinner G, Loustau D, Manca G, Matteucci G, Miglietta F, Ourcival JM, Papale D, Pilegaard K, Rambal S, Seufert G, Soussana JF, Sanz MJ, Schulze ED, Vesala T, Valentini R (2005) Europe-wide reduction in primary productivity caused by the heat and drought in 2003. *Nature* 437(7058):529–533
- Deslauriers A, Morin H (2005) Intra-annual tracheid production in balsam fir stems and the effect of meteorological variables. *Trees* 19(4):402–408
- Deslauriers A, Morin H, Urbinati C, Carrer M (2003) Daily weather response of balsam fir (*Abies balsamea* (L.) Mill.) stem radius increment from dendrometer analysis in the boreal forests of Québec (Canada). *Trees* 17(6):477–484
- Deslauriers A, Anfodillo T, Rossi S, Carraro V (2007) Using simple causal modeling to understand how water and temperature affect daily stem radial variation in trees. *Tree Physiol* 27(8):1125–1136
- Deslauriers A, Rossi S, Turcotte A, Morin H, Krause C (2011) Three-step procedure in SAS to analyze the time series from automatic dendrometers. *Dendrochronologia* 29(3):151–161
- Devine WD, Harrington CA (2011) Factors affecting diurnal stem contraction in young Douglas-fir. *Agric For Meteorol* 151(3):414–419
- Dong MY, Jiang Y, Wang MC, Zhang WT, Yang HC (2012) Seasonal variations in the stems of *Larix principis-rupprechtii* at the tree line of the Luya Mountains. *Acta Ecol Sin* 32(23):7430–7439
- Downes GM, Beadle C, Worledge D (1999) Daily stem growth patterns in irrigated *Eucalyptus globulus* and *E. nitens* in relation to climate. *Trees* 14(2):102–111
- Duchesne L, Houle D, Dorangeville L (2012) Influence of climate on seasonal patterns of stem increment of balsam fir in a boreal forest of Québec, Canada. *Agric For Meteorol.* 162–163:108–114
- Dufour B, Morin H (2013) Climatic control of tracheid production of black spruce in dense mesic stands of eastern Canada. *Tree Physiol* 33(2):175–186
- Ernst VDM, Marieke MT, Smiljanić M, Rossi S, Simard S, Wilmking M, Deslauriers A, Fonti P, Arx GV, Bouriaud O (2016) dendrometeR: analyzing the pulse of trees in R. *Dendrochronologia* 40:12–16
- Fritts HC (1976) *Tree Rings and Climate*. Academic Press, London
- Gou XH, Chen FH, Yang MX, Li J, Peng JF, Jin LY (2005) Climatic response of thick leaf spruce (*Picea crassifolia*) tree-ring width at different elevations over Qilian Mountains, northwestern China. *J Arid Environ* 61(4):513–524

- Gruber A, Baumgartner D, Zimmermann J, Oberhuber W (2009) Temporal dynamic of wood formation in *Pinus cembra* along the alpine treeline ecotone and the effect of climate variables. *Trees* 23(3):623–635
- Guan W (2007) A study on the growth of *Larix principis-rupprechtii* and the influence of water condition in the small watershed of Diediegou on the north side of Liupan Mountains. Doctoral Dissertation, Chinese Academy of Forestry, Beijing, China
- Gutiérrez E, Campelo F, Camarero JJ, Ribas M, Muntán E, Nabais C, Freitas H (2011) Climate controls act at different scales on the seasonal pattern of *Quercus ilex* L. stem radial increments in NE Spain. *Trees* 25(4):637–646
- Han XS, Wang YH, Yu PT, Xiong W, Li ZH, Cai JJ, Hao Xu (2019) Temporal and spatial variation and influencing factors of soil moisture in a *Larix principis-rupprechtii* plantation in semi-arid Liupan Mountains. *Northwest China J Soil Water Conserv* 33(1):111–117
- Herzog KM, Häslér R, Thum R (1995) Diurnal changes in the radius of a subalpine Norway spruce stem: their relation to the sap flow and their use to estimate transpiration. *Trees* 10(2):94–101
- Jiang Y, Zhang YP, Guo YY, Kang MY, Wang MC, Wang B (2015) Intra-Annual xylem growth of *Larix principis-rupprechtii* at its upper and lower distribution limits on the Luyashan Mountain in north-central China. *Forests* 6(12):3809–3827
- King G, Fonti P, Nievergelt D, Büntgen U, Frank D (2013) Climatic drivers of hourly to yearly tree radius variations along a 6 °C natural warming gradient. *Agric For Meteorol* 168:36–46
- Levanič T, Gričar J, Gagen M, Jalkanen R, Loader NJ, McCarroll D, Oven P, Robertson I (2009) The climate sensitivity of Norway spruce [*Picea abies* (L.) Karst] in the southeastern European Alps. *Trees* 23:169–180
- Li ZH (2014) The evapotranspiration of typical vegetation and the scale effect of the hydrologic features in slopes of Diediegou watershed of Liupan Mountains. Doctoral Dissertation, Chinese Academy of Forestry, Beijing, China
- Li XH, Liu R, Mao Z, Song Y, Liu L, Sun T (2014) Daily stem radial variation of *Pinus koraiensis* and its response to meteorological parameters in Xiaoxinganling Mountains. *Sheng Tai Xue Bao* 34:1635–1644
- Liu HX (2009) Study on effect of the climatic factors on the increment of *Larix principis-rupprechtii*. Master Dissertation, Hebei Agricultural University, Hebei, China
- Liu YH (2011) The characteristics of growth and carbon sequestration and water consumption in the small watershed of Xiangshuihe, Liupan Mountains. Doctoral Dissertation, Chinese Academy of Forestry, Beijing, China
- Liu ZB (2018) Spatio-temporal variations and scale transition of hydrological impact of *Larix principis-rupprechtii* plantation on a slope of Liupan Mountains, Doctoral Dissertation, Chinese Academy of Forestry, Beijing, China
- Liu HY, Williams AP, Allen CD, Guo DL, Wu XC, Anenkhonov OA, Liang EY, Sandanov DV, Yin Y, Qi ZH, Badmaeva NK (2013) Rapid warming accelerates tree growth decline in semi-arid forests of Inner Asia. *Glob Change Biol* 19(8):2500–2510
- Liu ZB, Wang YH, Tian A, Yu PT, Xiong W, Xu LH, Wang YR (2017a) Intra-annual variation of stem radius of *Larix principis-rupprechtii* and its response to environmental factors in Liupan mountains of northwest China. *Forests* 8(10):382
- Liu ZB, Wang YH, Xu LH, Liu Y, Deng XX, Wang YR, Zuo HJ (2017b) Temporal stability of soil moisture on a slope covered by *Larix principis-rupprechtii* plantation in Liupan Mountains. *J Soil Water Conserv* 31(1):153–165
- Liu ZB, Wang YH, Xu LH, Deng XX, Tian A (2018) Spatial-temporal variations and scale effect of soil moisture on *Larix principis-rupprechtii* plantation slope in semi humid Liupan Mountains, China. *Mountain Res* 36:43–52
- Lu M (2016) Monitoring radial growth of three conifer species in the eastern Qilian Mountains. Master Dissertation, Lanzhou University, Lanzhou, China
- Lu LH, He RM, Nong RH, Zhao ZG (2012) Effect of Slope Position on the Growth of *Mangli etia glauc*. *For Res* 25(6):789–794
- Lu M, Gou XH, Zhang JZ, Zhang F, Man ZH (2015) Seasonal radial growth dynamics of Qilian Juniper and its response to environmental factors in the eastern Qilian Mountains. *Quaternary Sci* 35(5):1201–1208
- Mencuccini M, Salmon Y, Mitchell P, Hölttä T, Choat B, Meir P, O'Grady A, Tissue D, Zweifel R, Sevanto S, Pfautsch S (2017) An empirical method that separates irreversible stem radial growth from bark water content changes in trees: theory and case studies. *Plant Cell Environ* 40(2):290–303
- Michelot A, Simard S, Rathgeber C, Dufrêne E, Damesin C (2012) Comparing the intra-annual wood formation of three European species (*Fagus sylvatica*, *Quercus petraea* and *Pinus sylvestris*) as related to leaf phenology and non-structural carbohydrate dynamics. *Tree Physiol* 32(8):1033–1045
- Oberhuber W, Gruber A, Kofler W, Swidrak I (2014) Radial stem growth in response to microclimate and soil moisture in a drought-prone mixed coniferous forest at an inner Alpine site. *Eur J For Res* 133(3):467–479
- Pantin F, Simonneau T, Muller B (2012) Coming of leaf age: control of growth by hydraulics and metabolics during leaf ontogeny. *New Phytol* 196(2):349–366
- Pärn H (2003) Growth of scots pine (*Pinus sylvestris*) on dunes of southwest Estonia related to climate. *For Ecosyst Coastal Dunes Southwest Estonia* 39:65–80
- Pérez CA, Carmona MR, Aravena JC, Fariña JM, Armesto JJ (2009) Environmental controls and patterns of cumulative radial increment of evergreen tree species in montane, temperate rainforests of Chiloé Island, southern Chile. *Austral Ecol* 34(3):259–271
- Pompa-García M, Sánchez-Salguero R, Camarero JJ (2017) Observed and projected impacts of climate on radial growth of three endangered conifers in northern Mexico indicate high vulnerability of drought-sensitive species from mesic habitats. *Dendrochronologia* 45:145–155
- Rossi S, Deslauriers A, Anfodillo T (2006) Assessment of cambial activity and xylogenesis by micro sampling tree species: an example at the Alpine timberline. *IAWA J* 27(4):383–394
- Rossi S, Deslauriers A, Anfodillo T, Carraro V (2007) Evidence of threshold temperatures for xylogenesis in conifers at high altitudes. *Oecologia* 152(1):1–12
- Shrestha KB, Chhetri PK, Bista R (2017) Growth responses of *Abies spectabilis* to climate variations along an elevational gradient in Langtang National Park in the central Himalaya, Nepal. *J For Res*. 1–8.
- Tardif J, Flannigan M, Bergeron Y (2001) An analysis of the daily radial activity of 7 boreal tree species. *Northwestern Québec Environ Monit Assess* 67(1–2):141–160
- Taschler D, Neuner G (2004) Summer frost resistance and freezing patterns measured in situ in leaves of major alpine plant growth forms in relation to their upper distribution boundary. *Plant Cell Environ* 27(6):737–746
- Tian QY, He ZB, Xiao SC, Peng XM, Ding AJ, Lin PF (2017) Response of stem radial growth of Qinghai spruce (*Picea crassifolia*) to environmental factors in the Qilian Mountains of China. *Dendrochronologia* 44:76–83
- Turcotte A, Morin H, Krause C, Deslauriers A, Thibeault-Martel M (2009) The timing of spring rehydration and its relation with the onset of wood formation in black spruce. *Agric For Meteorol* 149(9):1403–1409
- Vieira J, Rossi S, Campelo F, Freitas H, Nabais C (2013) Seasonal and daily cycles of stem radial variation of *Pinus pinaster* in a drought-prone environment. *Agric For Meteorol* 180:173–181

- Wang YB (2013) A study on the stem diameter variations and its response to environment factors for *Larix principis-rupprechtii* plantation in the semi-arid area of Liupan Mountains, northwest China. Master Dissertation, Inner Mongolia Agricultural University. Huhehaote, China
- Wang YN, Deng XX, Wang YH, Cao GX, Yu PT, Xiong W, Xu LH (2015a) The variation of biomass of *Larix principis-rupprechtii* plantation along slopes and its scale effect in the Xiangshuihe watershed of Liupan Mountains of China. *Ningxia For Res* 28(5):701–707
- Wang ZY, Yang B, Deslauriers A, Bräuning A (2015b) Intra-annual stem radial increment response of Qilian juniper to temperature and precipitation along an altitudinal gradient in northwestern China. *Trees* 29(1):25–34
- Wang WB, Zhang F, Yuan LM, Wang QT, Zheng K, Zhao CY (2016) Environmental factors effect on stem radial variations of *Picea crassifolia* in Qilian Mountains. *Northwestern China For* 7:210
- Xiao SC, Xiao HL, Si JH, Xi HY (2010) Study on the sub-diurnal radial growth of the *Populus euphratica*. *J Glaciol Geocryol* 32(4):816–822
- Xiao SC, Nie YQ, Wen F (2018) Seasonal dynamics of stem radial increment of *Pinus taiwanensis* Hayata and its response to environmental factors in the Lushan mountains. *Southeastern China For* 9:387
- Xiong W, Wang YH, Yu PT, Liu HL, Shi ZJ, Guan W (2007) Growth in stem diameter of *Larix principis-rupprechtii* and its response to meteorological factors in the south of Liupan Mountain. *China Sheng Tai Xue Bao* 27(2):432–440
- Zhang JZ (2018) Cambial phenology and intra-annual radial growth dynamics of conifers over the Qilian Mountains. Doctor Dissertation, Lanzhou University, Lanzhou, China
- Zhang RB, Yuan YJ, Gou XH, Zhang TW, Zhou C, Ji CR, Fan ZA, Qin L, Shang HM, Li XJ (2016) Intra-annual radial growth of Schrenk spruce (*Picea schrenkiana* Fisch. et Mey) and its response to climate on the northern slopes of the Tianshan Mountains. *Dendrochronologia* 40:36–42
- Zweifel R, Zimmermann L, Zeugin F, Newbery DM (2006) Intra-annual radial growth and water relations of trees: Implications towards a growth mechanism. *J Exp Bot* 57(6):1445–1459
- Zweifel R, Haeni M, Buchmann N, Eugster W (2016) Are trees able to grow in periods of stem shrinkage? *New Phytol* 211(3):839–849

Publisher's Note Springer Nature remains neutral with regard to jurisdictional claims in published maps and institutional affiliations.